Water Supply

IWA PUBLISHING

Water Supply Vol 22 No 5, 5206 doi: 10.2166/ws.2022.138

Vulnerability assessment of water resources in a karst mountainous area based on GIS/RS technology: a case study of Guiyang, Southwest China

Wei Li[a], Zulun Zhao[a], Sisi Lv[a], Weiquan Zhao[a,*] and Weici Su[a,b]

[a] Institute of Mountain Resource of Guizhou Province, Guiyang 550001, China
[b] College of Geography and Tourism, Key Laboratory of GIS Application, Chongqing Normal University, Chongqing 400047, China
*Corresponding author. E-mail: ZhaoWQ_2021@126.com

ABSTRACT

Water resource vulnerability in ecologically vulnerable karst areas is a key issue for regional sustainable development and the sustainable use of water resources. In this study, geographical information system (GIS) and remote sensing (RS) technology were employed to explore the vulnerability characteristics and spatial distribution of water resources in Guiyang City. The water resource vulnerability indicator in Guiyang ranged from 0.10 to 0.59, with an average value of 0.26. Yanglongsi Town, in Xifeng County, in the northern and main central urban area exhibited the highest water resource vulnerability, whereas Huaxi District in the south, and regions around Hongfeng Lake and Baihua Lake, in Qingzhen City, exhibited the lowest water resource vulnerability. Water resource vulnerability was predominantly mild, accounting for 35.85% of the total land area, followed by moderate (28.99%), with some non-vulnerable areas (13.60%) and very few extremely vulnerable areas (3.20%). Compared with traditional methods, the proposed index selection and assessment methods, based on GIS/RS, are both scientific and intuitive. In addition, the results are presented in detail, accurately reflecting the actual situation of water resource system vulnerability.

Key words: Guiyang City, karst, vulnerability, water resources

HIGHLIGHTS

- GIS spatial analysis technology was better in identifying the characteristics and spatial differences in water resource vulnerability than traditional assessment methods.
- The spatial distribution of water resources and water resource vulnerability in Guiyang is highly uneven.
- The water resource vulnerability index of Guiyang ranged from 0.10 to 0.59, and predominantly belonged to the mildly vulnerable category.

GRAPHICAL ABSTRACT

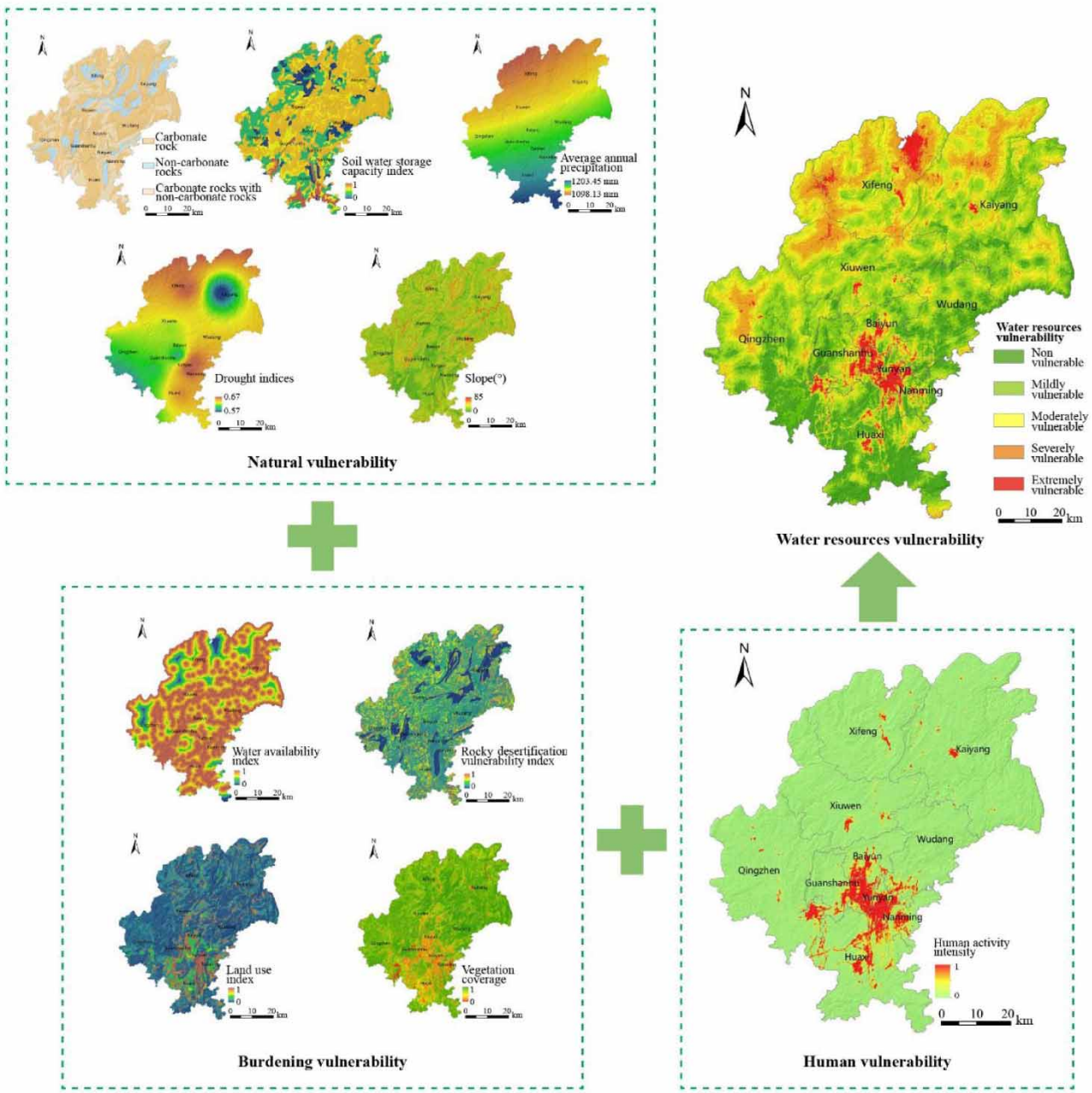

1. INTRODUCTION

Rapid development of the social economy has led to the remarkable expansion of urban boundaries and population, as well as deterioration of the natural environment, resulting in a series of problems such as a shortage of regional water resources and a decline in aquatic ecosystem quality (Zhang *et al.* 2009; Anandhi & Kannan 2018). Factors such as changes in the eco-environment and human activities have intensified the vulnerability of regional water resources, resulting in challenges to sustainable regional development (Li & Li 2012; Boruff *et al.* 2018). Thus, groundwater and water resource vulnerability has attracted considerable attention and become a key issue since Albinet and Margat first raised concerns regarding it in 1970 (Albinet & Margat 1970).

Since the inception of the 'International Conference on Soil and Groundwater Vulnerability' in 1987, scholars around the world have analyzed the vulnerability of water resources. For example, Brouwer and Falkenmark selected indicators to evaluate water resource vulnerability from the perspective of the regional water supply and demand balance (Brouwer & Falkenmark 1989). Muhammetoğlu *et al.* (2002) selected nine monitoring station indicators to evaluate the groundwater vulnerability of plains as a result of agricultural activities (Muhammetoğlu *et al.* 2002). Moreover, Rahman (2008) used GIS technology and a DRASTIC (Depth to water, Recharge, Aquifer media, Soil media, Topography, Impact of the vadose zone, Hydraulic conductivity) model to evaluate the vulnerability of regional water resources on the city scale. The results showed that more than 80% of water resources in the region considered were at a medium level or above (Rahman 2008).

Research on water resource vulnerability in China began in the 1990s (Qin *et al.* 2020). For example, Tang *et al.* (2000) discussed the concept, content, and technical methods implemented for water resource vulnerability assessment from the perspective of climate change. Ma & Gao (2003) selected related stress factors to evaluate the vulnerability of water resources in the southern margin of the Tarim Basin, revealing that most regions are in a vulnerable state. Furthermore, Zou *et al.* (2014) used the Hengyang Basin as an example, and combined GIS technology and the influence of human activities to analyze the vulnerability of regional water resource systems from a joint perspective.

Most of the above studies were conducted on watersheds, plains, basins, and their surroundings, which exhibited various degrees of limitations (Sun *et al.* 2016; Gao *et al.* 2019; Gui *et al.* 2021). There are relatively few studies on mountainous areas with complex climate and topography. As such, it is difficult to apply the current methods and indexes of assessment to karst areas. Karst regions exhibit peak-cluster depressions, peak-forest basins, with different shapes and sizes on the surface, and various types of dissolution gaps with underground karst caves, which form super-large natural reservoirs (Jones *et al.* 2019). This provides a large area for the stagnation and leakage of surface water resources, resulting in extreme difficulty in storing water on the surface. Conventional assessment methods and models do not consider factors such as surface water leakage, terrain fragmentation, shallow soil, and water intake. Moreover, most studies incorporate administrative divisions as the minimum assessment unit, and each administrative division unit consists of only one vulnerability result; this provides approximate results that cannot accurately reflect the spatial distribution of water resource vulnerability (Yao *et al.* 2020).

Therefore, grid-scale water resource vulnerability assessments are required to provide a more effective spatial analysis for regional water resource development and use. Although it is easy to obtain measured and statistical data in micro-regional water resource surveys and evaluations, the factors influencing water resource vulnerability in karst areas are complex and diverse. Moreover, there are currently no statistical or observational data on the vulnerability of water resources in karst areas. Furthermore, the traditional data analysis used to establish the assessment model cannot accurately reflect the spatial distribution and intrinsic nonlinear properties and laws of vulnerability (Zhou *et al.* 2007). Therefore, a new method based on geographical information system (GIS) and remote sensing (RS) technology is proposed in this study.

This study focuses on Guiyang City as an example to quantitatively evaluate grid-scale water resource vulnerability, with the help of GIS and RS technology. The aim of this assessment is to enrich research on urban water resources in karst mountainous cities and provide a decision-making reference for regional water resource system management, as well as the sustainable and rational use of regional water resources in similar regions.

Study area

Guiyang City is located in the centre of Guizhou Province, spanning the watershed zone between the Yangtze River Basin and the Pearl River Basin in China. Its geographical position lies between 106° 07′–107° 17′ N and 26° 11′–26° 55′ E. The dominant landform is inland karst mountains, with rugged and broken surfaces and significant vertical differences as well as an average altitude of approximately 1,100 m. It has a subtropical humid monsoon climate, with an average annual temperature of 14–16 °C and annual average precipitation of 1,129 mm.

2. DATA SOURCES

Data sources include the following: (1) The normalized difference vegetation index (NDVI). The data were calculated using Landsat 8-OLI satellite images, with a spatial resolution of 30 m. (2) Meteorological data, including annual average rainfall, average temperature, and hours of sunshine. (3) DEM (SRTM) data, with a spatial resolution of 30 m. (4) Soil type data derived from the 1:100,0000 soil database in China. (5) Spatial distribution data of rocky desertification in the study area from 2010. (6) Night light data from Luojia No.1 (LJ1-01) in 2019, with a spatial resolution of 130 m. (7) Land-use data with six categories: forest land, cultivated land, construction land, grassland, water areas, industrial and mining residential

land, with 25 secondary classifications. The entire data were clipped using the vector boundary of the study area, and uniformly converted into a WGS84/Albers Equal Area Conic projection for subsequent spatial calculation.

3. METHODS

In this study, GIS technology in combination with RS technology and the analytic hierarchy process (AHP) were used to study the vulnerability of regional water resources. AHP can effectively analyze and evaluate the non-sequential relationship between the target factors at different levels (Zhuang *et al.* 2003), which can generate practical and operable criteria for assessing the vulnerability of karst water resources. RS technology quickly and accurately acquires large-scale spatial environment data. Moreover, GIS technology achieves powerful spatial analysis and processing, and can deal with non-uniformity of the assessment index in space and time. Thus, this method has a great advantage in data processing.

Based on the actual situation of the study area, the characteristics of GIS technology, and the availability of data, 10 indicators were selected from the three aspects of natural vulnerability, burdening vulnerability, and human vulnerability of water resources (Nguyen *et al.* 2020). These indicators were used to construct a vulnerability assessment indicator system of water resources in Guiyang City, according to the principles of comprehensiveness, scientific validity, and feasibility. The assessment indicators include positive and negative indicators; positive indicators have a positive correlation with the vulnerability of water resources, whereas negative indicators have a negative correlation with the vulnerability of water resources. A comprehensive assessment of water resource vulnerability in Guiyang City was conducted by combining qualitative and quantitative methods.

After conducting the steps of spatialization and standardization for a single assessment indicator, the final assessment result was obtained by linear weighted super-position. The formula is as follows:

$$WRV = \alpha \times X1 + \beta \times X2 + \cdots + \delta \times Xi \tag{1}$$

where WRV is the regional water resource vulnerability indicator, $X1$, $X2$, and Xi are the standardized water resource vulnerability assessment indicators, and α, β, $\ldots$, δ are the corresponding weights of each indicator, respectively.

3.1. Karst distribution

Precipitation collects on the surface through confluence. Under the action of dissolution, erosion, and scouring of surface water, fissures and pores in the rocks become larger and more extensive; thus, the permeability of the rocks increases (Fang *et al.* 1993). The more significant the karst action, the greater the groundwater circulation. For example, in underground rivers and karst caves, serious infiltration of surface water (which is difficult to store) reduces the availability of surface water resources. However, the development and utilization of groundwater is challenging, resulting in serious water shortages in the region along with high vulnerability of carbonatite (a type of igneous rock which has a mineralogical composition of greater than 50% carbonate) mineral distribution areas. Thus, water resource vulnerability is highest in carbonate areas, moderate in mixed carbonate and non-carbonate areas, and relatively lower in non-carbonate areas. The karst distribution in the study area is shown in Figure 1.

3.2. Soil water storage capacity

Soil is the direct carrier of surface water and the main facilitator of water storage. A change in soil moisture is affected by many factors. In addition to being affected by precipitation, temperature, and cultivated crops, the water storage capacity of soils is also influenced by their physical and chemical properties, such as texture and organic matter content. In addition, the spatial difference of soil water storage capacity is large in karst mountain areas due to factors such as steep slopes and poor soil quality. The soil water storage capacity affects the potential storage capacity of water resources. Based on the 1:1 million soil database in China, this study compiled the soil records and research results of Zhou *et al.* (2007) and He *et al.* (2001), assigned values according to the water storage capacity of different soil types, and finally obtained the spatial distribution of soil water storage capacity in the study area, as shown in Figure 2(a).

3.3. Annual precipitation, drought indicator, and slope indicator

Precipitation is the direct source of surface water resources. The multi-year annual precipitation was derived using the monthly average data of 45 meteorological stations in the study area and its surroundings. GIS spatial interpolation was conducted to obtain the spatial distribution of annual precipitation over multiple years, as shown in Figure 2(c). The regional

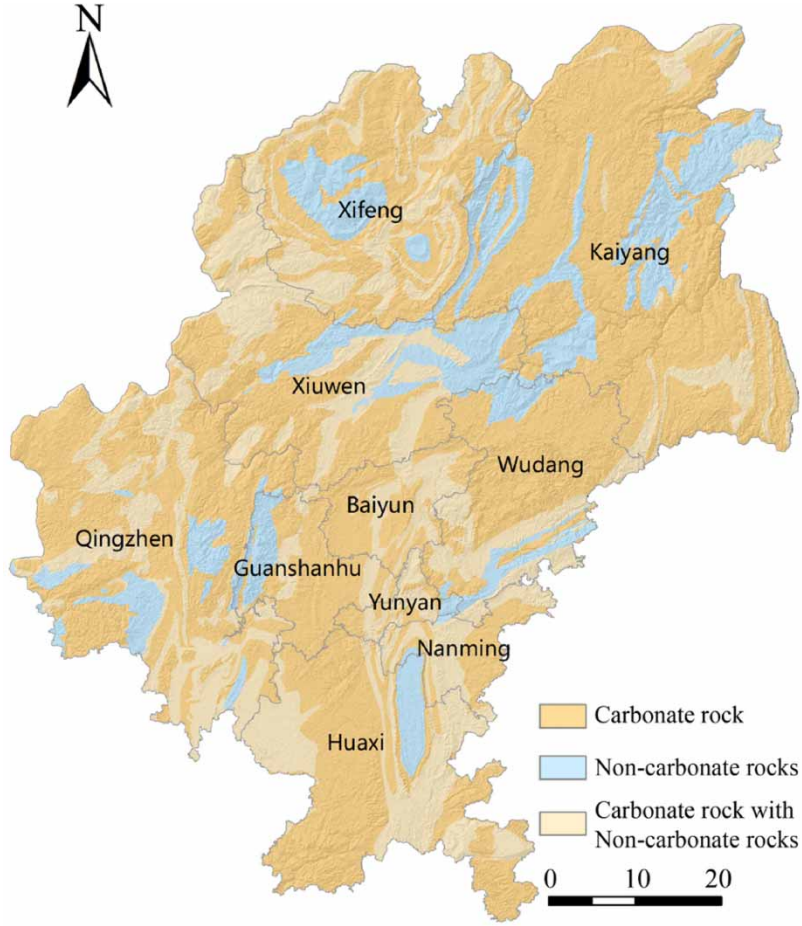

Figure 1 | Spatial distribution of karst geomorphology in the study area.

drought indicator was calculated using the research results of Zhuang *et al.* (2010) and Zhang *et al.* (2012). The formula is as follows:

$$S = PE/P \tag{2}$$

$$PE = k[10 \times T/\sum_{1}^{12}(0.09 \times T^{1.5})]^{(0.016\times\sum_{1}^{12}(0.09\times T^{1.5})+0.5)} \times \mu N/360 \tag{3}$$

where S indicates the drought indicator, PE indicates the evaporation capacity, P indicates the precipitation, T indicates the monthly average temperature, μ indicates the number of days per month, N indicates the monthly average sunshine hours, and k indicates the empirical coefficient, with a value of 16. The distribution of drought indicators in the study area is shown in Figure 2(b). The slope was extracted from SRTM 30-m DEM data, as shown in Figure 3.

3.4. Water resource availability indicator

Theoretically, water resources located closer to the surface are easier to extract. Considering factors such as high topographic relief, steep slopes, broken terrain, and other factors, the lakes, rivers, and reservoirs have been incorporated from the current land-use data with a 500 m buffer area. Thus, the shorter the straight-line distance from the buffer area, the higher the water resource availability indicator. Conversely, the farther the distance from the 500 m buffer zone, the more difficult it is to access the water and the lower the water resource availability indicator. Using the ArcGIS spatial analysis function, the linear distance between each raster point outside the buffer zone and the water source in the buffer zone of 500 m was

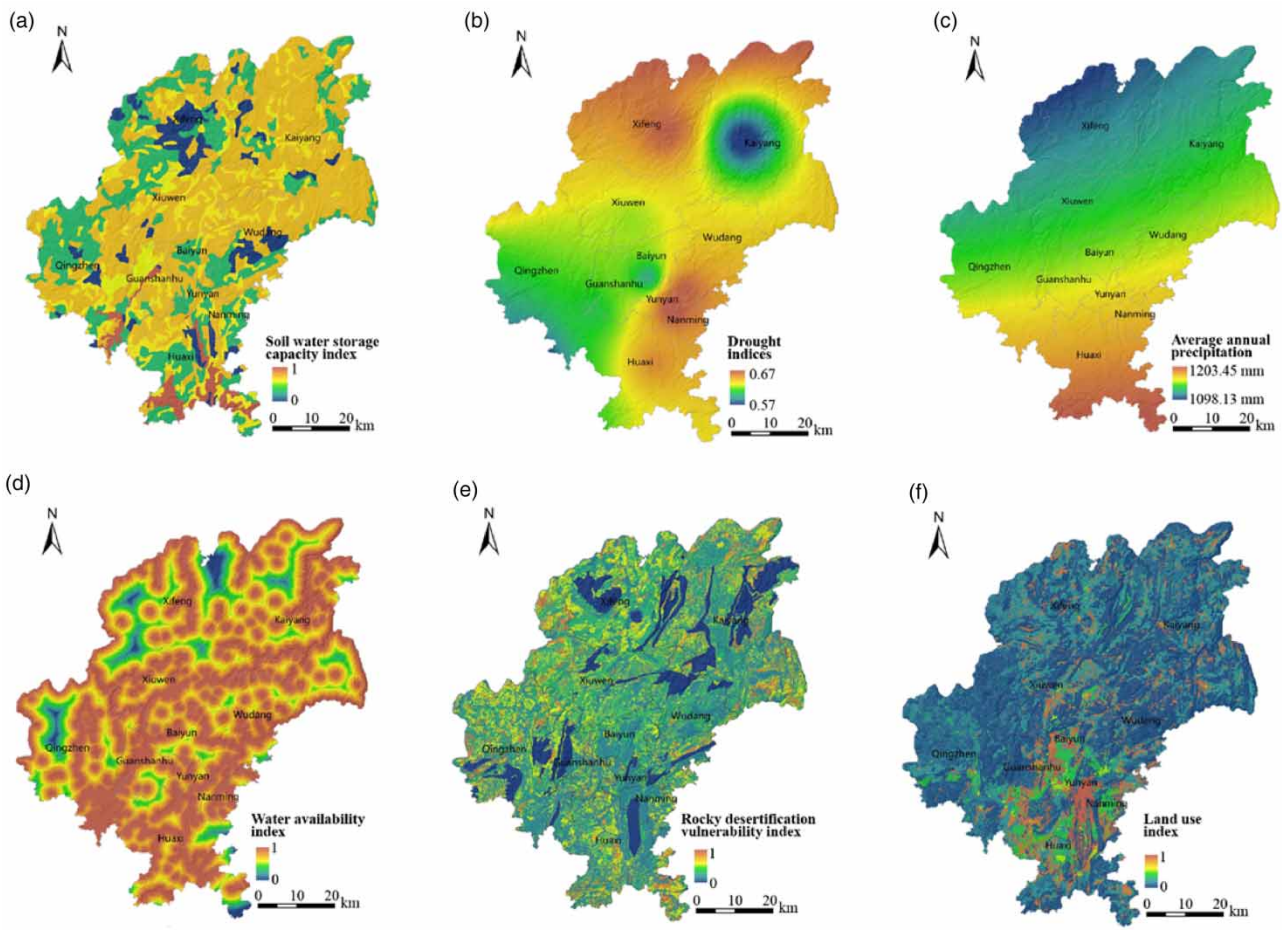

Figure 2 | Spatial distribution of (a) soil water storage capacity, (b) drought indices, (c) multi-year average precipitation, (d) water resource availability indicator, (e) rocky desertification vulnerability, and (f) land-use indicator in the study area.

calculated after converting the data into raster format. The data space was standardized to construct a spatial distribution map of the water resource availability indicator for the study area (Figure 2(d)).

3.5. Rocky desertification vulnerability indicator

An increase in rocky desertification will lead to fewer water resources and greater vulnerability of the water resources. Based on the investigation of rocky desertification data, its intensity was determined according to the degree of its dependence on water resources in the non-karst area. Thus, non-rocky, potentially rocky, lightly rocky, moderately rocky, severely rocky, and intensely rocky desertification areas were assigned the values of 0.1, 0.2, 0.3, 0.5, 0.7, 0.9, and 1, respectively. The higher the score, the higher the vulnerability of water resources. The spatial distribution of the rocky desertification vulnerability indicator in the study area is shown in Figure 2(e).

3.6. Land-use indicator

The change in land-use structure is an important factor affecting the regional eco-system, the circulation of material and energy, and the vulnerability of water resources. It is also the main driver of short-term regional hydrological changes. To a certain extent, it destroys the natural pattern and evolution process of regional primitive water resource circulation, causing a change in the spatial distribution of regional water resource quantity and water quality. Spatial change is one of the main factors influencing water resource vulnerability and also exerts serious pressure on freshwater systems (Li *et al.* 2002; Abera *et al.* 2019). Due to the increased demand of different land-use types for water resources, as well as the characteristics of land-use types in the study area (Figure 2(f)), the water resource vulnerability weight of different land-use types was determined in combination with expert advice. The weight values are listed in Table 1.

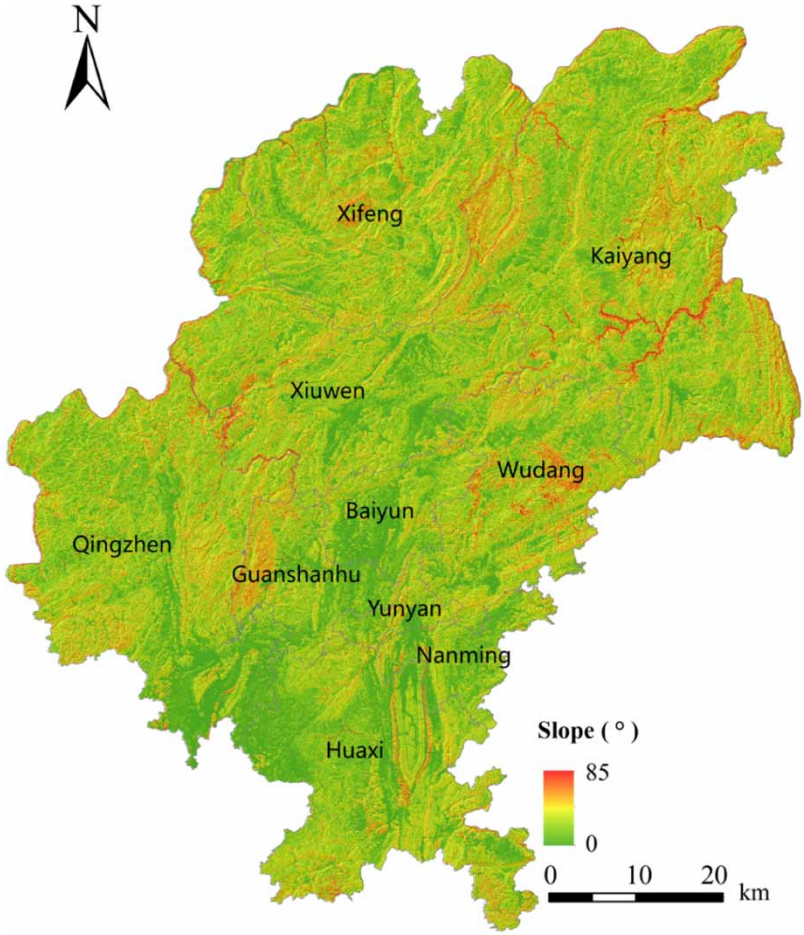

Figure 3 | Spatial distribution of slopes in the study area.

Table 1 | Weights of land-use types

Primary land-use type	Weight	Secondary land-use type	Weight
Woodland	0.06	Woodland	0.01
		Bushland	0.01
		Sparse woodland	0.02
		Other woodland	0.02
Cultivated land	0.23	Paddy field	0.20
		Dryland	0.03
Water area	0.04	Rivers and canals	0.14
		Lakes	0.01
		Reservoirs, pits, and ponds	0.25
Construction land	0.51	Urban land	0.33
		Rural settlement	0.11
		Other construction land	0.07
Grassland	0.15	High coverage grassland	0.03
		Medium coverage grassland	0.04
		Low coverage grassland	0.08

3.7. Vegetation coverage

Vegetation coverage is a key bridge linking surface and underground ecological processes. It is also an intuitive reflection of global climate and hydrological changes, which play a key role in regional climate regulation, water conservation, and the global carbon cycle (Li *et al.* 2014). Vegetation growth is closely related to changes in regional water resources and is also an intuitive reflection of regional water resource vulnerability. The NDVI vegetation indicator was calculated using 2019 Landsat 8-OLI images, and the vegetation coverage indicator of the study area (Figure 4) was calculated according to the following formula:

$$f = \frac{(NDVI - NDVImin)}{(NDVImax - NDVImin)} \tag{4}$$

where *NDVI* is the normalized vegetation indicator, which is defined as the difference between the values of the near infrared band and the visible red band and the ratio of the sum of the values of the two bands, and *NDVI max* and *NDVI min* are the maximum and minimum values of *NDVI*, respectively.

3.8. Intensity indicator of human activity

Human interference with water resources has always been a key research topic in many disciplines, such as hydrology, geography, and ecology (Wang *et al.* 2006; Lin *et al.* 2009). The higher the population density, the stronger the intensity of human activity and the greater the demand and vulnerability associated with water resources. In terms of spatial distribution, population density is the most intuitive manifestation of social and economic activities and urban expansion of

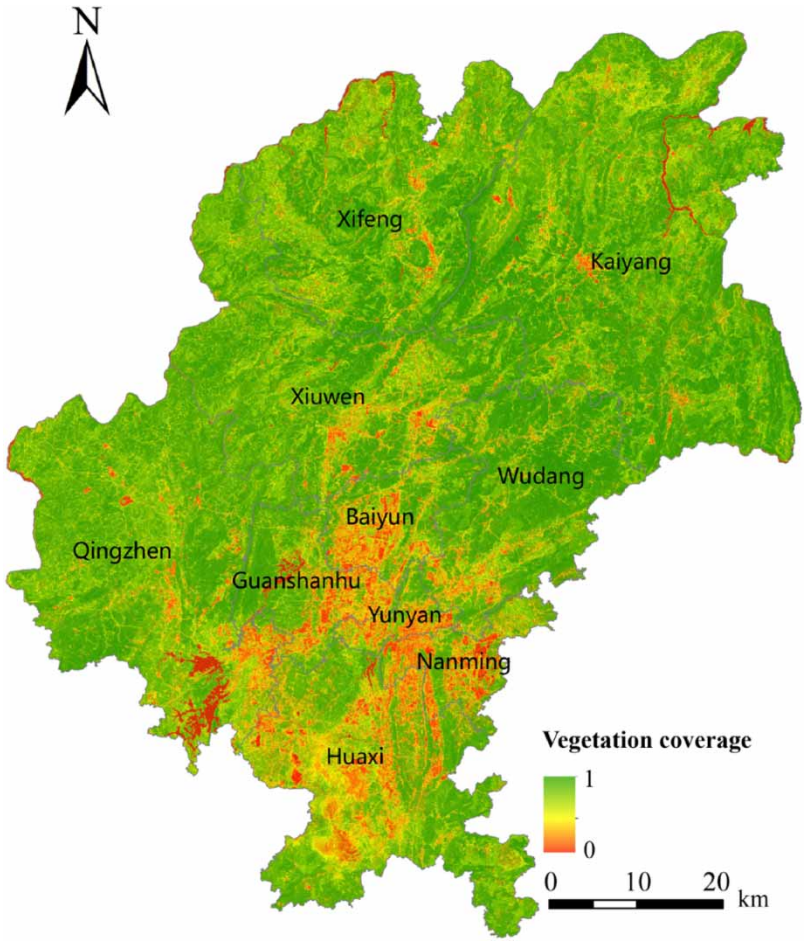

Figure 4 | Spatial distribution of the vegetation cover indicator in the study area.

humans. A previous study found that night-time light data are closely related to human activities and has been widely used in various fields of study related to human activities (Pan & Li 2016; Wang *et al.* 2019; Zhong & Liu 2019). In this study, the night-time light data of the Luojia-1 satellite (LJ1-01) from 2019 were used as the data source to simulate the intensity of human activities (Figure 5).

4. RESULTS

4.1. Comprehensive assessment of water resource vulnerability

To facilitate the use of each indicator in the calculation of results, 10 assessment factors were initially rasterized by the GIS spatial analysis function. Each raster unit forms a basic spatial calculation unit, and each indicator data standard was spatially normalized. In the normalization process, the forward indicator is normalized in the forward direction, and the reverse indicator is normalized in the reverse direction. The specific standardization formula is as follows:

Forward normalization:

$$X = (Xi - Xmin)/(Xmax - Xmin) \tag{5}$$

Reverse standardization:

$$X = 1 - (Xi - Xmin)/(Xmax - Xmin) \tag{6}$$

where X is the normalized parameter value of the indicator layer, Xi is the initial parameter value of the indicator layer, and Xmax and Xmin are the maximum and minimum values of the indicator layer, respectively. After normalization, each

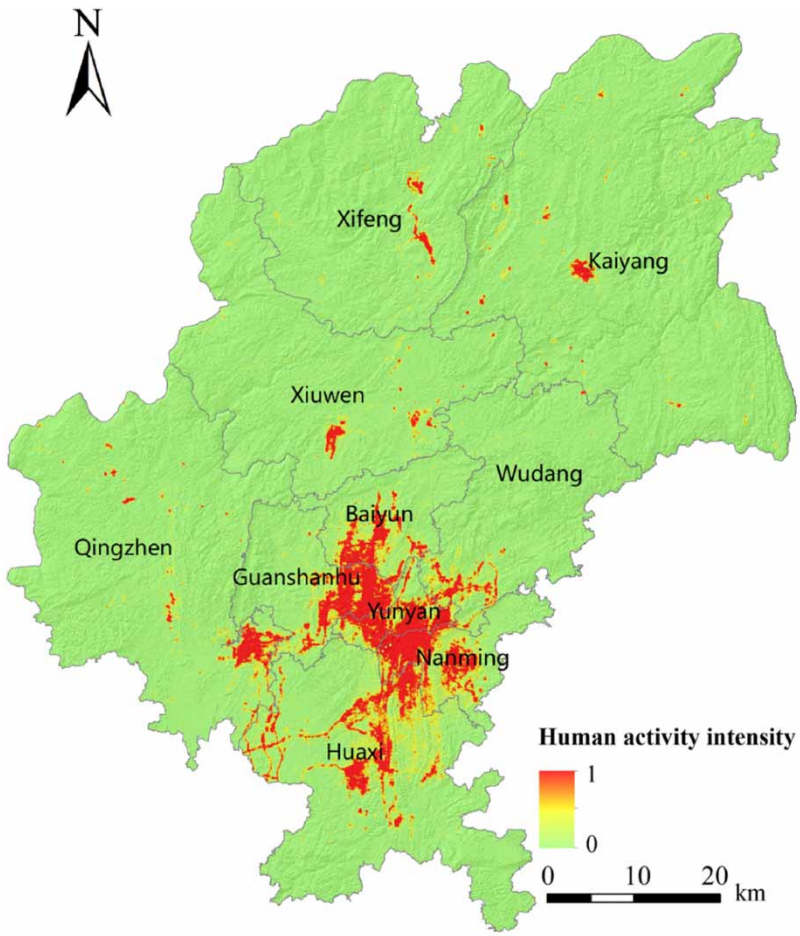

Figure 5 | Spatial distribution of human activity intensity in the study area.

assessment indicator adopts a GIS spatial weighted superposition mode, and the vulnerability indicator of water resources in the study area is obtained. The natural breakpoint method was divided into five categories, which were successively divided into five sub-categories: non-vulnerability, mild vulnerability, moderate vulnerability, severe vulnerability, and extreme vulnerability. The assessment indicator weight was determined by referring to the unique characteristics of the region, combining expert consultation and the AHP, and passing the consistency test ($CR < 0.01$). The weight values are shown in Table 2. Finally, the spatial distribution map of water resource vulnerability in the study area (Figure 6) and the area distribution of each vulnerable area (Table 3) were obtained.

4.2. Assessment results

According to Tables 3 and 4, and Figure 6, the study area exhibits characteristics of good water resources in the northern and middle areas, and poor water resources in the southern area. Thus, there is a clear spatial variation in water resource vulnerability. Within the study area, mildly vulnerable areas account for the largest proportion, followed by moderately vulnerable areas, non-vulnerable areas, and severely vulnerable areas. However, extremely vulnerable areas represent the smallest proportion. These areas are described in more detail below.

Non-vulnerable areas: These areas have a water resource vulnerability indicator value between 0.12 and 0.22 and account for an area of 1,474.48 km^2. This region has the lowest vulnerability to water resources and is mainly distributed in the southern Huaxi District and the surrounding areas of Hongfeng Lake and Baihua Lake in Qingzhen City, with the rest distributed in Wudang District and Kaiyang County. The areas of Huaxi District and Wudang District, which are not vulnerable, account for 52 and 33% of the total land area of their respective districts and counties. Among each district and county, Huaxi District and Qingzhen City have the largest proportion of non-vulnerable areas, accounting for over 300 km^2 and 55.91% of the total non-vulnerable area in the study area. These non-vulnerable areas are rich in water resources, with relatively flat terrain, dense vegetation coverage, strong water conservation capacity, rich precipitation, and low water demand. The major component of water is used for agricultural irrigation, with strong water resources guaranteeing adequate capacity and sufficient water resources per capita.

Mildly vulnerable areas: Areas with a water resource vulnerability indicator value between 0.22 and 0.26 represent 2,880.49 km^2 and are predominantly distributed in the Wudang District, Xiuwen County, Kaiyang County, and Qingzhen City (three counties and one city), where the area of mildly vulnerable areas is above 300 km^2. The total area of mildly vulnerable areas in this region accounts for 73.15% of the total area of mildly vulnerable locations in the entire study area and 55.75% of the total land area of the three counties and one city. Kaiyang County has the largest area, comprising 790.10 km^2, and Yunyan District and Nanming District exhibit the smallest areas of 20.79 km^2 and 69.23 km^2 respectively, with other districts and counties being above 100 km^2.

Moderately vulnerable areas: These areas have a water resource vulnerability indicator value between 0.26 and 0.31 and represent an area of 2,329.45 km^2. They are mainly distributed in three counties and one city, in the study area (Xifeng County, Kaiyang County, Xiuwen County, and Qingzhen City). The moderately vulnerable areas in these locations represent 758.08 km^2, 434.97 km^2, 371.01 km^2, and 358.84 km^2, respectively, accounting for 37.44, 41.99, 34.62, and 26.00% of the

Table 2 | Water resource vulnerability assessment indicator weights

Indicator	Weight
Karst spatial distribution	0.04
Soil water storage capacity indicator	0.07
Average annual precipitation	0.13
Drought indicator	0.07
Slope indicator	0.08
Water resource availability indicator	0.17
Rocky desertification vulnerability indicator	0.04
Land-use indicator	0.15
Vegetation coverage	0.07
Human activity intensity indicator	0.18

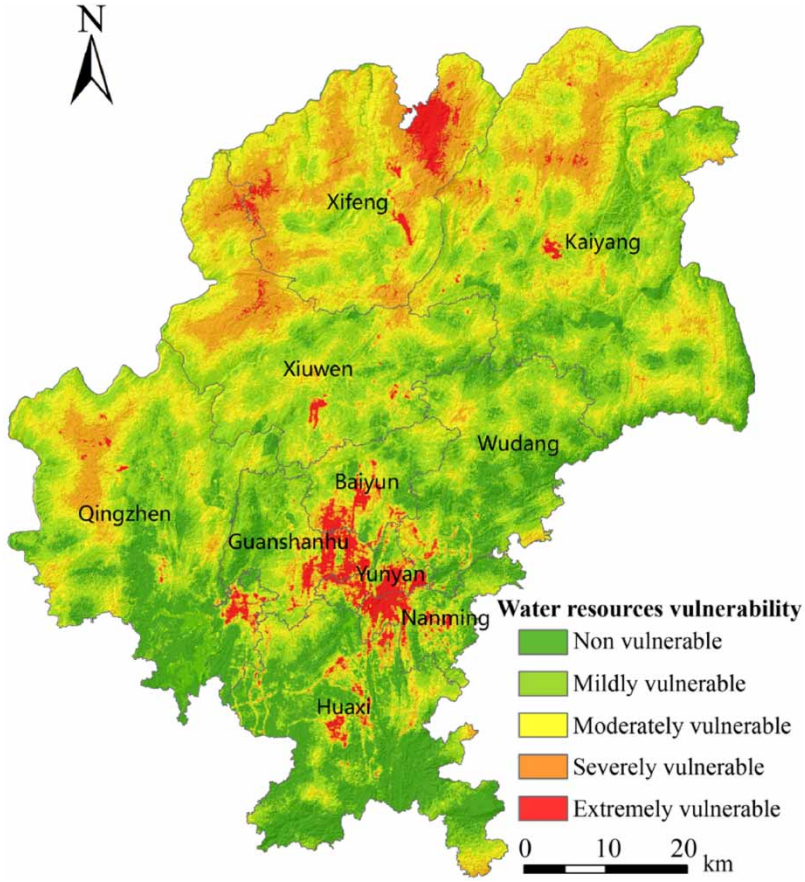

Figure 6 | Spatial distribution of water resource vulnerability in the study area.

Table 3 | Results of water vulnerability assessment in the study area

Vulnerability category	Vulnerability indicator value	Description of water resource vulnerability	Area (km^2)	Proportion (%)
Non-vulnerable	0.10–0.22	Rich water resources, abundant precipitation, less water demand, strong storage capacity, abundant per capita water resources	1,474.47	18.35
Mildly vulnerable	0.22–0.26	Humid climate with more precipitation, less evaporation, sparse population.	2,880.49	35.85
Moderately vulnerable	0.26–0.31	Some natural restrictions on water resources, general difficulty accessing water, outdated basic water conservation facilities.	2,329.45	28.99
Severely vulnerable	0.31–0.37	Lack of water resources, poor guaranteed capacity, large consumption capacity, poor storage capacity	1,092.87	13.60
Extremely vulnerable	0.37–0.59	Extremely vulnerable water resources, poor recycling capacity, high consumption, serious engineering water shortage, difficult water intake, dense population.	256.71	3.20

district and county area, respectively. Less than 50 km^2 each of Yunyan District and Nanming District are moderately vulnerable, i.e., 15.06 km^2 and 34.58 km^2, respectively. The spatial distribution of this category is relatively scattered, with moderately vulnerable areas distributed in the areas surrounding cities and towns. The water demand is predominantly for agricultural and industrial use.

Severely vulnerable areas: These areas have a water resource vulnerability indicator value between 0.31 and 0.37 and comprise 1,092.87 km^2 of the study area. They are mainly distributed in Liuchang Miao Township in the west of Qingzhen City,

Table 4 | Assessment results of water vulnerability in each district and county in the study area

District/County	Non-vulnerable (km^2)	Mildly vulnerable (km^2)	Moderately vulnerable (km^2)	Severely vulnerable (km^2)	Extremely vulnerable (km^2)	Total
Huaxi District	495.43	280.30	122.75	43.88	15.45	957.81
Wudang District	223.06	331.04	107.81	18.79	3.03	683.73
Yunyan District	10.00	20.79	15.06	18.33	27.82	92.00
Nanming District	52.47	69.23	34.58	21.93	29.93	208.14
Baiyun District	37.65	115.07	66.42	29.73	21.73	270.60
Guanshanhu District	58.60	118.79	59.93	31.51	40.03	308.86
Xiuwen County	64.05	430.13	371.01	190.53	15.96	1,071.68
Kaiyang County	199.57	790.10	758.08	265.33	11.74	2,024.82
Xifeng County	4.66	168.96	434.97	351.48	75.88	1,035.95
Qingzhen City	328.98	556.08	358.84	121.36	15.14	1,380.40
Total	1,474.47	2,880.49	2,329.45	1,092.87	256.71	8,033.99

Liuguang, Dashi, and Liutong Township in the northwest of Xiuwen County, Jiuzhuang Town, Xiaozhaiba Town, and Wenquan Town in Xifeng County, and Fengsan Town, Machang Town, and Zhaiji Township in Kaiyang County. The severely vulnerable parts of these areas account for 84.98% of the total severely vulnerable area throughout the study area. Xifeng County and Kaiyang County have the largest severely vulnerable areas, reaching 351.48 km^2 and 265.33 km^2, respectively, accounting for 32.16 and 24.28% of the severely vulnerable areas in Guiyang City, whereas Yunyan District and Wudang District have the smallest areas, at only 18.33 km^2 and 18.79 km^2, respectively. As the regional surface fluctuates greatly, karst action is strong, water resources are scarce, the guaranteed capacity is poor, the consumption capacity is large, and the storage capacity is poor.

Extremely vulnerable areas: These areas have a water resource vulnerability indicator value between 0.37 and 0.59, and an area of 256.71 km^2. They are mainly distributed in the Nanming District, Yunyan District, Guanshanhu District, Baiyun District, and Yanglongsi Town of Xifeng County in Guiyang City. Among these districts and towns, the total extremely vulnerable area, in the four districts of the main city (Nanming District, Yunyan District, Guanshanhu District, and Baiyun District), is 119.51 km^2, accounting for 46.55% of the total extremely vulnerable area. Thus, the pressure on water resources in urban areas is significantly higher than the average level of the study area. Secondary and tertiary industries in the main urban area and its surroundings are relatively developed with highly intensive human activities. In 2018, the total GDP in the four districts of the main urban area accounted for 53.92% of the total GDP in the whole city. The total population accounted for 47.18% of the total population in Guiyang City, and the population density was 2,896.97 people/km^2, far higher than the average level of 606.95 people/km^2 for Guiyang City. A large amount of productive and domestic water resulted in huge water consumption, resulting in extremely vulnerable water resources.

5. DISCUSSION

The empirical study shows that it is feasible to assess the vulnerability of water resources on a grid scale. Moreover, this study achieved an effective expression of the spatial distribution of regional water resource vulnerability. The main characteristics of the spatial variability of regional water resource vulnerability in the study area are as follows:

(1) The high vulnerability of water resources in areas with intensive human activities is mainly due to the influx of a large number of people from districts, counties, villages, and rural areas since the 21st century, with an obvious acceleration of urbanization and a highly concentrated urban population. Population agglomeration forces large areas of newly constructed land to expand into areas surrounding the city and changes the original land-use/cover structure of the region. With the development of the social economy, both water consumption by tertiary industries and domestic use increases rapidly, whereas the total amount of regional water resources remains relatively constant. This leads to a very severe situation for regional water resources.

(2) Under constant rainfall conditions, rocks are continuously weathered under the action of rainwater dissolution. Geomorphic features such as karst caves, underground rivers, and dissolved crevices are formed, and the soil in rocky desertification areas turn barren. The soil types are mainly mountain red soil, yellow soil, and lime soil. Loose and porous sandy loam evaporates vigorously, resulting in a poor regional water holding capacity, high precipitation infiltration intensity with infiltration rates greater than 95%. Most of the precipitation is infiltrated underground. Groundwater is difficult to extract where slopes exceed angles of 25° in mountainous areas. Under the same precipitation conditions, slope runoff is a direct source of water flow. The higher the slope, the greater the concentration of rainfall, the faster the down flow speed, and shorter the time of confluence on the slope. In addition to the small amounts of water stored in soil and vegetation, a large amount of running water flows out through gravitational potential energy, formed by the slope, and flows into rivers and lakes, resulting in a large total amount of regional water resources. This results in a small amount of available water resources per capita, and complex water utilization, which are the main factors for large spatial differences in water resource vulnerability in the study area.

Most traditional vulnerability assessment methods are based on administrative divisions, regardless of their size, generating single assessment results. Therefore, the results do not reflect the spatial difference in regional water resource vulnerability. By contrast, this study uses GIS spatial analysis to quantitatively study the vulnerability of water resources in Guiyang City on a grid scale from three aspects: natural, environmental, and man-made. Therefore, the assessment results are more detailed and accurate than traditional assessment results based on administrative regions.

6. CONCLUSIONS

The assessment results reflect better characteristics and spatial differences in water resource vulnerability than those obtained using traditional assessment methods, thereby providing a theoretical basis and decision support for the rational utilization and scientific planning of regional water resources. The key findings are as follows:

(1) The water resource vulnerability index of Guiyang ranged from 0.10 to 0.59, and predominantly belonged to the mildly vulnerable category, which accounted for 35.85% of the study area, followed by moderately vulnerable (28.99%), non-vulnerable (18.35%), severely vulnerable (3.60%), and extremely vulnerable (3.20%). Among the districts and counties, four areas (Yunyan District, Xiuwen County, Kaiyang County, and Xifeng County) exhibited moderate vulnerability or above (moderate + severe + extreme) in more than 50% of the total land area.

(2) The spatial distribution of water resources and water resource vulnerability in Guiyang is highly uneven; there is a substantial difference between the northern and the southern areas. The major vulnerable urban areas are the north of Kaiyang County, the north of Xifeng County, the north of Xiuwen County, the west of Qingzhen City, and areas surrounding these main urban areas. The distribution of productive forces and population does not match the distribution of water resources. Therefore, water supply and demand are extremely unbalanced, and the influence of human activities is the major factor leading to high vulnerability of water resources. Other highly vulnerable areas are mainly caused by natural factors such as a large number of slopes, difficulty of water intake and conservation, and other harsh natural conditions. The south and centre of Wudang districts in Kaiyang County, the north of Baiyun District, the east of Qingzhen City, and the south of Huaxi District possess low water resource vulnerability, low population density, and superior natural environments, with water resources being predominantly used for agriculture.

(3) The influencing factors of water resource vulnerability in different regions are variable. The main factors affecting the water resource vulnerability in the central part of the study area are ranked as follows: the human activity intensity indicator (population density or water demand) has the strongest impact, followed by the water resource availability index, followed by the land use type index, and the other factors index has the weakest influence. In the north of the study area such as Xifeng and Kaiyang County, the main influencing factors are ranked as follows: the first is water resource availability, the second is the soil water storage capacity indicator, the third is the average annual precipitation, and the last is the other factors. In the south of the study area such as Huaxi area, water resource availability dominates. It is followed by average annual precipitation and human activity intensity. The other factors have the weakest impact. In brief, human activity intensity (population density) and water resource availability have a greater influence on regional water resource vulnerability.

Compared with traditional methods, the results of this study are more detailed and accurate. However, due to the limited availability of data, some relevant assessment indicators have been omitted. Moreover, in terms of the spatial distribution characteristics of water resource vulnerability, the present study did not involve an analysis of the spatial-temporal evolution or a quantitative analysis of the factors influencing the evolution of water resource vulnerability in the study area. Therefore, future research should attempt to obtain high-precision data, optimize the determination of assessment indicators and weight methods, and verify the results of this study.

ACKNOWLEDGEMENTS

This research was funded by the Basic Research Program of Guizhou Province (Qiankehe Foundation [2018]1418), the Guizhou Provincial Science and Technology Projects (Qiankehe support [2018]2806) analysis and interpretation of data and the Youth Fund of the Guizhou Academy of Sciences (Grant number [J] [2021]25).

DATA AVAILABILITY STATEMENT

All relevant data are included in the paper or its Supplementary Information.

REFERENCES

Abera, W., Tamene, L., Abegaz, A. & Solomon, D. 2019 Understanding climate and land surface changes impact on water resources using Budyko framework and remote sensing data in Ethiopia. *Journal of Arid Environments* **167**, 56–64.

Albinet, M. & Margat, J. 1970 Mapping of groundwater pollution vulnerability. *Bull. BRGM 2ème 2nd Series* **3** (4), 13–22.

Anandhi, A. & Kannan, N. 2018 Vulnerability assessment of water resources – translating a theoretical concept to an operational framework using systems thinking approach in a changing climate: case study in Ogallala Aquifer. *Journal of Hydrology* **557**, 460–474.

Boruff, B., Biggs, E., Pauli, N., Callow, N. & Clifton, J. 2018 Changing water system vulnerability in Western Australia's wheatbelt region. *Applied Geography* **91**, 131–143.

Brouwer, F. & Falkenmark, M. 1989 Climate-induced water availability changes in Europe. *Environmental Monitoring and Assessment* **13** (1), 75–98.

Fang, J. F., Lin, J. S., Li, J. Z. & Zhang, Y. G. 1993 Relation of solution to environment in Karst Area – a case study of Hongshui River Basin. *Acta Geographica Sinica* **60** (2), 122–130.

Gao, C., Liu, L., Ma, D., He, K. Q. & Xu, Y. P. 2019 Assessing responses of hydrological processes to climate change over the southeastern Tibetan Plateau based on resampling of future climate scenarios. *Science of the Total Environment* **664**, 737–752.

Gui, Z. H., Chen, X. H. & He, Y. H. 2021 Spatiotemporal analysis of water resources system vulnerability in the Lancang River Basin, China. *Journal of Hydrology* **601** (12), 126614.

He, F. H., Huang, M. B. & Li, J. B. 2001 Role of soil water reservoirs and forests in regulating water resources. *Soil and Environmental Sciences* **10** (1), 42–44.

Jones, N. A., Hansen, J., Springer, A. E., Valle, C. & Tobin, B. W. 2019 Modelling intrinsic vulnerability of complex karst aquifers: modifying the COP method to account for sinkhole density and fault location. *Hydrogeology Journal* **27**, 2857–2868.

Li, C., Gao, J. & Cao, H. 2002 The status and trend of research on the impact of land use change on water resources. *Soil* **4**, 191–196.

Li, J. & Li, L. 2012 Water resources supporting capacity to regional socio-economic development of China. *Acta Geographica Sinica* **67** (3), 410–419.

Li, Q., Zhou, D. & Chen, X. 2014 The accumulation, decomposition and ecological effects of above-ground litter in terrestrial ecosystem. *Acta Ecologica Sinica* **34** (14), 3807–3819.

Lin, X., Fang, Y., Liao, Z. & Chen, H. 2009 Impact of global warming and human activities on groundwater temperature. *Journal of Beijing Normal University (Natural Science)* **45**, 452–457.

Ma, J. & Gao, Q. 2003 Groundwater vulnerability and its assessing method in the arid land of NW China. *Arid Land Geography* **26** (1), 44–49.

Muhammetoğlu, H., Muhammetoğlu, A. & Soyupak, S. 2002 Vulnerability of groundwater to pollution from agricultural diffuse sources: a case study. *Water Science and Technology* **45** (9), 1–7.

Nguyen, T. T., Ngo, H. H., Guo, W. S., Nguyen, H. Q., Luu, C., Dang, K. B., Liu, Y. W. & Zhang, X. B. 2020 New approach of water quantity vulnerability assessment using satellite images and GIS-based model: an application to a case study in Vietnam. *Science of the Total Environment* **737**, 139784.

Pan, J. & Li, J. 2016 Estimate and spatio-temporal dynamics of electricity consumption in China based on DMSP/OLS images. *Geographical Research* **35**, 627–638.

Qin, J., Ding, Y. J., Zhao, Q. B., Wang, S. P. & Chang, Y. P. 2020 Assessments on surface water resources and their vulnerability and adaptability in China. *Advances in Climate Change Research* **11**, 381–391.

Rahman, A. 2008 A GIS based DRASTIC model for assessing groundwater vulnerability in shallow aquifer in Aligarh, India. *Applied Geography* **28** (1), 32–53.

Sun, S. K., Wang, Y. B., Liu, J., Cai, H. J., Wu, P., Geng, Q. L. & Xu, L. J. 2016 Sustainability assessment of regional water resources under the DPSIR framework. *Journal of Hydrology* **532**, 140–148.

Tang, G., Li, X. & Liu, Y. 2000 Assessment method of vulnerability of water resources under global climate change. *Advances in Earth Science* **15** (3), 313–317.

Wang, G., Xia, J., Wang, D. & Ye, A. 2006 A distributed monthly water balance model for identifying hydrological response to climate changes and human activities. *Journal of Natural Resources* **21** (1), 86–91.

Wang, Y., Shui, W. & Yang, H. 2019 Temporal and spatial evolution of human landscape development in the Fujian delta urban agglomeration in the 21st century: based on energy-GIS approach. *Acta Ecologica Sinica* **39** (5), 208–220.

Yao, L., Shuai, Y. & Chen, X. 2020 Regional water system vulnerability evaluation: a bi-level DEA with multi-followers approach. *Journal of Hydrology* **589** (3), 125160.

Zhang, L., Xia, J. & Hu, Z. 2009 Situation and problem analysis of water resource security in China. *Resources and Environment in the Yangtze Basin* **18** (2), 116–120.

Zhang, X., Xiong, L., Lin, L. & Long, H. 2012 Application of five potential evapotranspiration equations in Hanjiang Basin. *Arid Land Geography* **35**, 229–237.

Zhong, L. & Liu, X. 2019 Application potential analysis of LJ1-01 new nighttime light data. *Bulletin of Surveying and Mapping* **7**, 132–137.

Zhou, J., Yang, Y., Tian, Y. & Xie, X. 2007 Concept and assessment on vulnerability of agricultural water resource in hilly area of southern China. *Journal of Natural Resources* **22**, 302–310.

Zhuang, L., Xie, Z. & Shen, W. 2003 A new method that can improve regional eco-environmental evaluation-combining GIS with AHP. *Resources and Environment in the Yangtze Basin* **12**, 163–168.

Zhuang, X., Yang, S., Zhao, Z. & Zhang, L. 2010 Drought index and its application in the analysis on drought monitoring in Altai Region Xinjiang. *Journal of Catastrophology* **25** (3), 81–85.

Zou, J., Zhang, W. & Yang, Y. 2014 Evaluation of water resources system vulnerability in southern hilly rural region based on the GIS/RS take Hengyang Basin as an example. *Scientia Geographica Sinica* **34** (8), 1010–1017.

First received 7 December 2021; accepted in revised form 26 February 2022. Available online 18 March 2022